Activity Descriptor for Catalytic Reactions on Doped Cerium Oxide

M. Aryanpour,[†,‡,]* A. Khetan,[‡] and H. Pitsch[†,‡]

[†]Department of Mechanical Engineering, Stanford University, Stanford, California 94305
[‡]Institut für Technische Verbrennung, RWTH Aachen University, Templergraben 64, 52056 Aachen, Germany

S *Supporting Information*

ABSTRACT: It is well-known that ceria enhances chemical activity and catalyst durability in several important catalytic reactions, including CO oxidation and NO_x reduction. Of great practical value is then having a theoretical model to predict the effect of doping on the ceria activity before the actual synthesis of its compounds. Such a model is developed in the present work on the basis of experimentally observed data, where we verify our hypothesis that the energy for oxygen vacancy formation is a simple yet powerful activity descriptor for this class of materials. We further benchmark and use our DFT + U computations to estimate this descriptor and to suggest a few transition metals that would increase the activity of ceria toward redox reactions. This new activity descriptor might be an important factor in similar systems because it does not require any knowledge about the exact chemistry or mechanism of catalysis.


KEYWORDS: *cocatalysis, ceria, catalytic activity, activity descriptor, theoretical modeling*
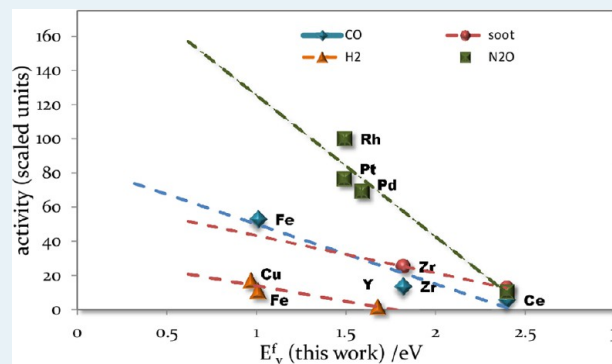
1. INTRODUCTION

Ceria and ceria-derived materials have found widespread usage in industrial catalytic reactions both as active participants and as support for other active materials. Common examples include the water-gas shift (WGS) reaction[1] in fuel cells, preferential CO oxidation (PROX) reaction,[2,3] and three-way catalysis (TWC) processes for automotive exhaust gas purification.[4,5] Ceria-based materials are also potential candidates for high-temperature catalytic applications because they remain largely unaffected by carbon deposition when used as an anode with hydrocarbon fuels.[6] These materials are also known to stabilize precious metal dispersion and prevent their sintering, thus enhancing the durability of the catalyst.[7−9]

The promoting role of ceria in catalytic reactions used to be attributed to merely causing a better dispersion of known catalyst elements or alloys on the ceria surface.[10] Today it is well established that ceria itself also participates actively in the chemistry via a redox process,[11] in which it releases or absorbs an O atom, depending on the reaction conditions, particularly on the partial pressure of oxygen. For instance, in TWC processes, where the catalyst is exposed to cyclically varying stoichiometric composition of reactants in the feed, ceria assists in the removal of CO by donating oxygen under oxygen lean conditions according to the reaction

$$CeO_2 + xCO \rightarrow CeO_{2-x} + xCO_2 \tag{1}$$
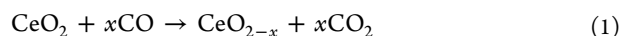
and aids the conversion of NO under oxygen-rich conditions according to the reaction

$$CeO_{2-x} + xNO \rightarrow CeO_2 + 0.5xN_2 \tag{2}$$
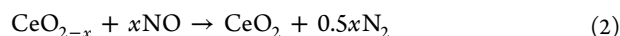
Creation of an O vacancy leads to a defect site in the pure CeO_2 crystal or surface while the oxidation state of one Ce atom changes reversibly, in a formal sense, from a 4+ to 3+. From an electronic structure point of view, the ground state electronic structure of CeO_2, the occupancy of the 4f electrons has been a subject of debate for a long time.

Early experimental studies using spectroscopy[12] and measurements of optical reflectivities[13] suggested that mixed or intermediate valence states with partially occupied 4f states could be ruled out for CeO_2. Later experimental investigations of the electronic structure of CeO_2 surfaces using TPD and XPS[14] indicate that in the presence of defects, the 4f state in Ce^{3+} is occupied and accompanied by diffusion of O vacancies from the bulk to the surface.[15] More recent studies employing STM conductance spectroscopy (see ref 16 and references therein) as well as a combined STM−DFT approach[17,18] point out that the localization of the excess electrons in the 4f states of Ce is due to the creation of O vacancies. Localization of excess electrons on Ce 4f orbitals upon O vacancy formation in turn influences the ordering of energy levels of the occupied 4f states of reduced Ce ions and their coordination with other atoms because a higher coordinated Ce^{3+} ion is less stable.[19] These factors ultimately determine the stability and energy of formation of O vacancies, which is shown in the present work to play the role of an activity descriptor.

In the literature, the activity of CeO_2 is often discussed in terms of its oxygen storage capacity (OSC), which is directly related to the energy required to form an oxygen vacancy, denoted by E_v^f. The facile uptake and release of O atoms in doped CeO_2 enables it to directly participate in catalytically relevant processes, such as CO oxidation[2,20] and NO_x[21] reduction. It has been observed that doping of CeO_2 with rare-earth and transition metals enhances its redox properties in addition to creating a high surface area and active sites for chemical reactions. Dopants such as Cu,[22] Zr,[22,23] Fe,[23] Zn,[23] Mn,[24] Co,[24] Ru,[25] Rh,[25,26] Pt,[24−26] and Pd[24−26] exhibit synergistic redox behavior when supported on CeO_2.

In addition to experimental studies, a great volume of theoretical work using first principles calculations has been performed on CeO_2 in both its doped and undoped forms. Apart from Hartree−Fock (HF)[27] and ionic potential (IP)[28] calculations, density functional theory (DFT) has been extensively used for studying bulk and low index surfaces of undoped CeO_2. Several computational studies[29−34] have shown that the two standard flavors of DFT calculations, namely, the local density approach (LDA) and the generalized gradient approach (GGA) in their original form, fail to predict the correct electronic states of the reduced Ce atom owing to the lack of cancellation of the Coulomb self-interaction. The reason for this failure lies in the occupation of 4f states in Ce^{3+} whose strongly correlated electrons are not captured by the conventional exchange-correlation functionals.

Several modeling studies of CeO_2 doped with metals such as Zr,[35−38] Ru,[37,38] Ni,[38−40] Pd,[38−42] Pt,[38,40,42,43] Ir,[38,44] Au,[38,45,46] Rh,[38,43] Y,[37,47] La,[37,47] Ta,[48] and Nb[48] have been performed using first principles calculations to examine the promoting effect of dopants in CeO_2. Wang et al.[36] used DFT + U calculations for finding the O vacancy formation energy of $Ce_xZr_{1−x}O_2$ solid solutions for different values of x. They proposed that structural relaxation determines the overall trends for E_v^f and strongly depends on the ionic radius of the dopant element. Scanlon et al.[42] performed a DFT analysis of Pd and Pt-doped CeO_2 and found a large displacement of the dopant ions from the Ce lattice site because both Pd(2+) and Pt(2+) prefer to adopt a square-planar (d^8) coordination. This effect was explained as a result of the crystal field stabilization of dopant ions, which have a lower coordination number in their own oxide structure than in the host oxide, thus leading to creation of under-coordinated O atoms that are readily removable in the host oxide upon doping.

Nolan[39] used hybrid DFT and DFT + U simulations to study the (111) and (110) surfaces of CeO_2 doped with divalent cations. He proposed that O vacancies form spontaneously to compensate for the dopant oxidation state such that Pd and Ni can maintain their square planar coordination environments. In another study of the trivalent cation-doped (110) CeO_2 surface,[47] the most stable defect depended on the ionic radius of the dopant. It was also observed that a large mismatch in the ionic radius of the dopant and the host oxide atom left the host oxide structure rather unfavorably distorted. Krcha et al.[38] recently made a computational study on periodic trends of oxygen vacancy formation for surface layer O vacancies by doping the CeO_2 (111) surface with various transition metal elements and found that the C−H bond activation in dissociative methane adsorption over doped ceria is correlated with its surface reducibility.

Despite such a large amount of experimental and computational work on ceria, a clear structure−activity relationship at a theoretical and modeling level is missing from the current literature. Theoretical modeling of doped CeO_2 also is not intrinsically a straightforward task because of fundamental uncertainties regarding the oxidation state, morphology, size, and distribution of dopant elements on the CeO_2 substrate. Such factors obscure the actual contribution of the CeO_2 support to the total catalytic activity of the material.[45]

In this work, we try to clarify the effect of ceria as a cocatalyst and to fill a part of that theoretical modeling gap. First, we consider three main scenarios in which ceria might affect chemistry in a catalytic system. Focusing on the dominant case, we benchmark our DFT calculations, where a good general agreement with the literature is reached, in particular in estimating the E_v^f values when CeO_2 is doped with different transition metals. This agreement ensures our next discussions and conclusions will remain valid whether the literature values or the results of our calculations are used for E_v^f. Next, we verify our hypothesis with the help of measured data from literature that the activity of all considered doped CeO_2 materials, to the extent of our survey, indeed correlates well with its corresponding E_v^f value. Data have been gathered for several catalytic reactions, such as CO, soot, and N_2O conversion. The presented activity descriptor is based on a consistent set of calculations, unlike the potentially inconsistent results in the literature. Finally, we apply this activity descriptor to predict the effect of various transition metals—Cu, Fe, Zn, Zr, Ru, Rh, Pt, Pd, Y, and Ir—on the activity of CeO_2.

2. THEORY AND COMPUTATIONAL METHOD

2.1. Theoretical Modeling. The meaning of doping in the current literature is attributed to a broad range of structures and categorizations in mixing dopant and doped materials. For instance, dopants can be added to CeO_2 to form isolated phases in which they can retain main features of their bulk crystal having a distinct phase boundary with the host, as shown in Figure 1a. Alternately, the dopant atoms can replace Ce atoms in various configurations, such as in bulk CeO_2, on an extended surface, at some interstitial locations, or otherwise vacant crystalline sites as pictured in Figure 1b. In yet another setting, the dopant can be deposited in the form of ordered thin films, clusters, or monolayers (Figure 1c) with CeO_2 acting as a support material. In such cases, the actual chemistry, which occurs on the deposited doping layers, can be affected through the interaction of these layers with the substrate; here, CeO_2.

We note that the above three scenarios are just simplified pictures or models of more complex situations that occur in practice. The dispersion, shape, and size of the dopant in real catalyst materials depend upon preparation conditions and synthesis procedures.[41] The actual catalyst material can be a mixture of all such simple cases, or may even contain more complicated structural topologies. Instead of dealing with complicated models, our categorization of different scenarios in Figure 1 enables us to isolate roles of major players of cocatalysis that are manifested primarily in the topology of a synthesized catalyst.

Cases a and c, as shown in Figure 1, represent schematic situations of doping CeO_2 that may or may not be achieved, depending on the synthesis route. Case b, in contrast, reflects a more common situation because irrespective of the employed synthesis method, a few or several of the dopant atoms could penetrate from the substrate surface to the extent of a few atomic layers within the CeO_2 lattice. This case also represents one of the most widely studied systems owing to its relative
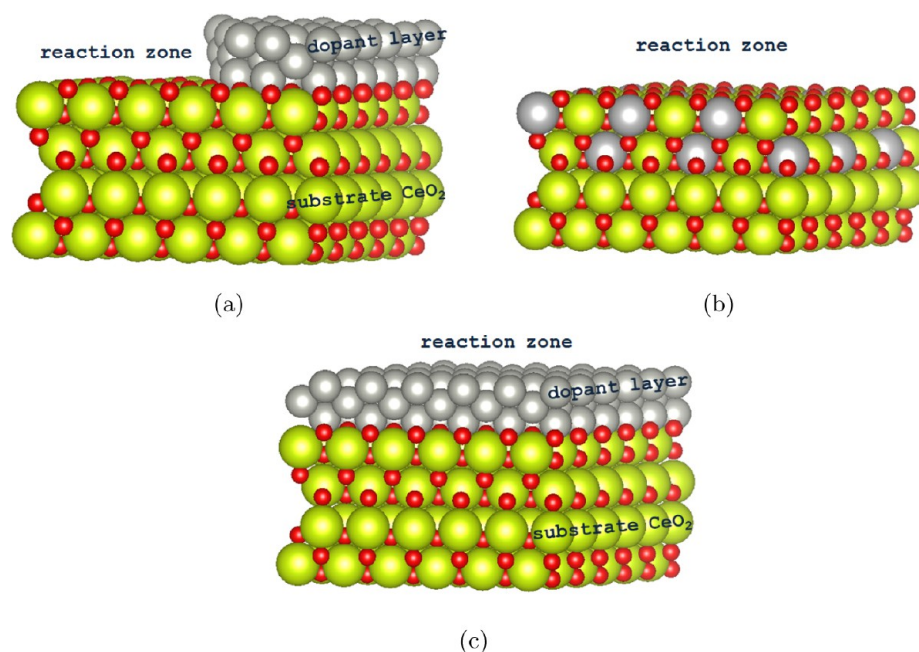
Figure 1. Simple configurational scenarios in doping CeO$_2$: (a) a mixture of CeO$_2$ and dopant crystal acting as an isolated phase, (b) Ce ion replaced by dopant, and (c) dopant deposited as overlayers on CeO$_2$.

simplicity from the point of view of periodic calculations. Obviously, there is hardly any escape from the condition in which a few dopant atoms either replace a Ce ion or could locate themselves in the interstices or defects of the CeO$_2$ crystalline structure. For these reasons, we choose case b as the first model system to be studied by replacing a Ce atom with a dopant element in a slab model CeO$_2$.

At the same time, we understand that one might consider or be dealing with two or all of the three cases instead of only case b. More important is then the question of which scenario dominates the catalytic activity if it does. Our above argument to focus on case b does not intend to reduce the importance of the other cases. Rather, we are suggesting a model and a hypothesis in which using case b can explain and predict experimental trends. The relation of this model system to the activity of doped ceria is explored below.

It is our goal here to find a theoretical parameter or measure for quantifying the activity of ceria as a catalyst or cocatalyst. We seek a metric that can distinguish various compounds in a relative sense if not necessarily in an absolute classification. To this end, one should first look at experimental results, although experimental studies aimed at measuring activity are highly application-specific and contingent to variable reaction conditions.

In our survey of recent literature, it was found that the measured values for the oxygen storage capacity (OSC) of CeO$_2$ are rather scattered with respect to its chemical activity. Therefore, we set aside OSC and utilize the energy required for oxygen vacancy formation (E_v^f) as the activity descriptor. In addition, the OSC of a material has a bulk nature, whose reported value is an average over all possible different local properties and, therefore, hard to calculate if not impossible at all. In contrast, vacancy formation is a local phenomenon, which makes it easy to model and to estimate its energetics. We show in this work how the choice of E_v^f as a descriptor leads to a unified picture for the activity of ceria versus doping elements. It may be argued that the catalytic activity of ceria is caused by other factors, such as the structure distortions or the coordination mismatches. We are not setting aside such factors but show, instead, that the E_v^f can capture the major trends.

2.2. Comparison of DFT Calculations for CeO$_2$. We perform periodic density functional calculations within the DFT + U framework to describe pure and doped CeO$_2$, as well as the (111) and (110) surfaces of undoped CeO$_2$. The first reason to calculate E_v^f in this work, instead of directly using available literature data, is to base the conclusions on a set of fully consistent results. As is discussed below, a few parameters, such as U and location of vacancy, are known to affect computations in general and, in particular, those corresponding to CeO$_2$. Using a set of literature data, which have been obtained by inconsistent computational settings, would have rendered the validity of the conclusions questionable. Second, from a predictive point of view, it was necessary to develop a uniform computaional plan to study those doping elements not considered in the literature yet. Thus, both the development of a consistent computational method and performing the calculations could have not been skipped in this work.

The quantum mechanical modelings in this paper use the VASP[49] code for the DFT + U with generalized gradient approximation Perdew–Burke–Ernzerhof (GGA-PBE) functionals.[50,51] The cutoff energy is 500 eV unless otherwise mentioned. The choices for the other parameters, such as K-points sampling, the U value, and the cell size, are mentioned for each stage separately.

Most computational parameters, such as U and the superiority of hybrid-DFT versus DFT + U, seem widely studied in the literature. That is not, however, very true for cerium compounds. The current literature lacks a *well-established* or *well-agreed* setting to compute E_v^f in doped ceria. For this material, in particular, one has to choose or decide on

- the value of U for Ce,
- which crystallographic surface is the most stable or relevant for chemical activity,

- if the DFT + U results change the surface preference compared with more accurate results of hybrid-DFT, and
- the location of the oxygen vacancy when computing E_v^f.

This paper tries to address those issues before suggesting the activity descriptor based on computations.

In general, the DFT + U approach significantly improves the description of reduced CeO_2 with respect to DFT, but it suffers from the dependence on U_{eff} because no single value of U_{eff} can correctly reproduce all properties, such as the surface reaction energy, lattice parameter, and band gap, simultaneously.[52] Various authors have used U_{eff} values between 2 and 7 eV to correctly predict physical observables (see refs 30,34, and 53 and references therein). In addition, the type of projector functionals affects the exact choice of U_{eff}.[31] An acceptable U_{eff} for all computations is still lacking, and at the moment, a semiempirical value should be used instead.

We compare our results with respect to surface relaxations and energies calculated using the DFT and hybrid-DFT approach available in the literature.[39] Similar to U in the DFT + U formalism, hybrid-DFT calculations also depend on parameters such as screening length and percentage of HF exchange. These parameters comparatively have more established values, at least for oxides, particularly in the case of CeO_2 as used in refs 39,54, and 55. This justifies using them as a comparison for the DFT + U calculations presented here.

CeO_2 has a cubic fluorite structure in the bulk phase with a unit cell belonging to the space group $Fm-3m$. The model of bulk used for the calculations contains 4 units of CeO_2 initially arranged in a perfect $Fm-3m$ lattice symmetry. The modeled crystal consists of 4 face-centered Ce atoms with 8 O atoms located within the cell in the tetrahedral interstices (Figure 2).
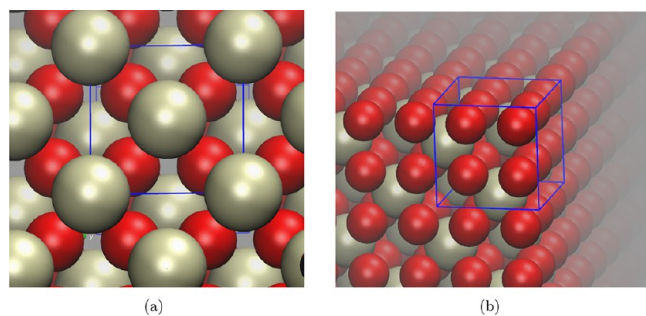

Figure 2. Structure of bulk ceria crystal: (a) the (100) surface and (b) isomeric view (the smaller spheres represent oxygen atoms, and the larger ones are cerium atoms).

The coordination number of each O atom is 4, and each Ce atom, in turn, is coordinated with 8 O atoms. Now we consider the surface energy of ceria. The (111) CeO_2 surface is type II, according to the Tasker classification of surfaces.[56] Experimental studies using techniques such as STM,[57,58] AFM,[59] ion scattering spectroscopy,[60] and low energy electron diffraction,[61] conclude that the (111) CeO_2 surface is terminated by oxygen atoms. For the present calculations, the Ce atoms on the layers are arranged in 2 × 2 configurations, leading to 16 formula units, that is, 48 atoms in the model. The supercell is isolated from its periodic images by an ~10 Å vacuum space along the z direction, which points in the [111] direction. Figure 3 illustrates our model for the (111) surface, consisting of four CeO_2 trilayers.

The (110) CeO_2 surface has also been studied by STM and RHEED techniques,[62] in which the terminated layers were
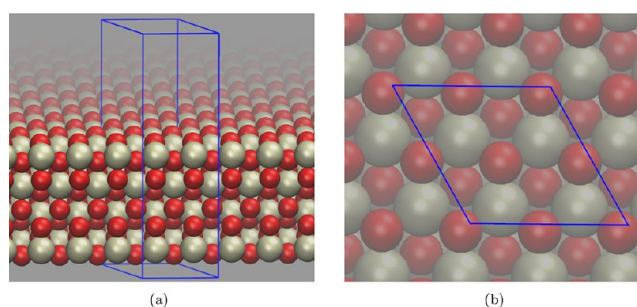

Figure 3. Theoretical model to compute the (111) surface energy: (a) side view and (b) top view (the smaller spheres represent oxygen atoms, and the larger ones are cerium atoms).

found to be stoichiometric. Our model for the (110) surface in Figure 4 has 6 trilayers, each arranged in a 2 × 1 structure.
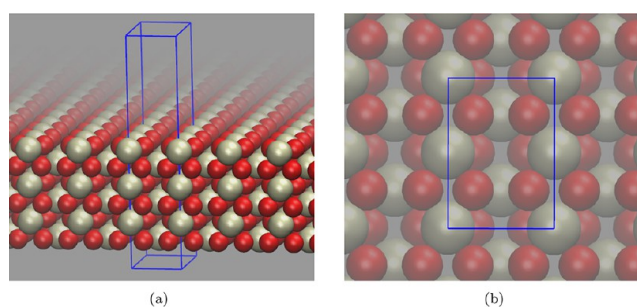

Figure 4. Structure of computational model for (110) surface energy: (a) side view and (b) top view (the smaller spheres represent oxygen atoms, and the larger ones are cerium atoms).

An empty space of ~14 Å separates each surface from its periodic images in the [110] direction. The supercell thus contains 36 atoms in 12 formula units of CeO_2. The anion terminated (100) surface is comparatively the most unstable,[58] because cleaving this surface gives rise to a dipole moment in the normal direction.[63] The same result has been confirmed in recent DFT calculations (see ref 30 and references therein), and hence, (100) is left out from the rest of our investigations.

The calculations for surface energy and relaxation values for undoped CeO_2 in this work were done by relaxing all atomic degrees of freedom using the conjugate gradient algorithm to reach the ground state as implemented in VASP.[49] The volume and shape of the unit cell were allowed to vary during calculations. A fixed 4 × 4 × 4 K-points sampling was applied for the bulk structures on Monkhorst pack grids in the Brillouin zone, and the parameter U was varied in the range 2−5 eV. The lattice constant value of 5.402 Å for bulk CeO_2 calculated in this work is very close to the measured value of 5.41 Å[64] and was not relaxed, but kept the same. Ionic relaxations were allowed for all the atoms belonging to the top two layers. The cutoff energy was set to 500 eV using the PBE functional for exchange-correlation effects. The relaxations were stopped if both the change in the total free energy and in the eigenvalues energy between two steps were smaller than 10^{-3} eV.

We calculated the stability of the (111) and (110) surfaces to further benchmark our DFT + U settings. In Figure 5, we compare the surface energy of the (111) and (110) structures calculated by our DFT + U with those of the HSE06 functional used by Nolan.[39] The HSE06 method has been reported to be
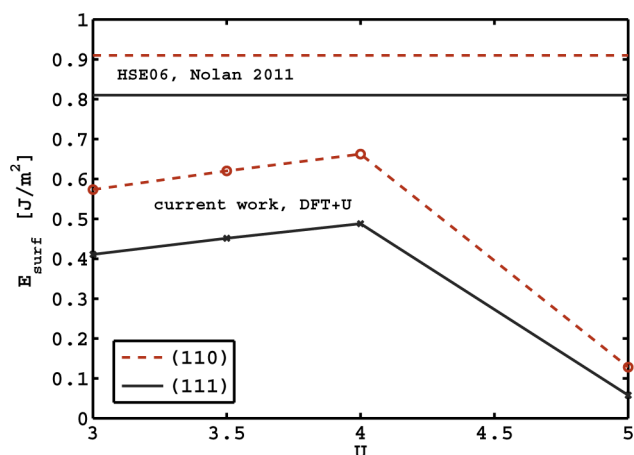
Figure 5. Surface energy of the (111) and (110) structures of CeO$_2$ calculated using models shown in Figures 3 and 4.

Figure 6. Computational model consists of 2 × 2 × 4 trilayers of ceria with the dopant metal atom shown in blue (The smaller spheres represent oxygen atoms, and the larger ones are cerium atoms.).

more accurate, yet computationally much more expensive than DFT + U. It is beneficial, then, to benchmark the less expensive DFT + U against the more reliable HSE06 method. Figure 5 reveals that both methods agree on the stability of the (111) surface relative to the (110) surface: 0.1 J m^{-2} in HSE06, and 0.07−0.17 J m^{-2} in DFT + U, depending on U. The stability trend does not vary with the exact value of the parameter U, although the difference in surface energy decreases when U is increased from 4 toward 5 eV. At U = 5 eV, our calculated difference in surface energy, 0.07 J m^{-2}, equals a similar result reported in ref 39 using DFT + U.

It must be noted that reliable experimental data for relaxed surfaces of CeO$_2$ are not available in recent literature, whereas all comparisons for surface energies show only qualitative trends. In addition, we calculated surface relaxations for the (111) and (110) surfaces. Our results indicate small surface relaxations: less than 0.1 Å inward and ~0.2 Å outward the bulk for the (111) and (110) surfaces, respectively, which are in good agreement with the previously reported trends from DFT + U calculations by Nolan et al.[30]

In the case of CeO$_2$ doped with transition metals, we applied computational settings similar to those used in the case of undoped CeO$_2$. In each case, four O−Ce−O trilayers of atoms were considered for calculations, thus consisting of a total of 12 layers of atoms. Each trilayer was arranged in a 2 × 2 structure using a slab model for the (111) CeO$_2$ surface, as shown in Figure 6. The dopant replaces a Ce atom in the second trilayer, that is, the fifth atomic layer from the vacuum direction. The main reason to select the second Ce layer and not the first or the other two is to keep the electronic perturbation caused by doping close to the location of the oxygen vacancy. Although the optimum position may vary depending on the doping element, it is maintained at the second Ce layer to preserve the consistency of computations.

To determine the position of the first O vacancy in a slab model (Figure 7a) for the (111) surface in a 3 × 3 × 4 trilayer configuration, we calculated the E_v^f values as a function of the O layer containing the vacancy. Figure 7b shows that the most energetically favorable layer to contain an O vacancy is the second O layer, or the subsurface that is just below the skin. The third O layer comes out to be as favorable as the second if a cutoff energy of 300 eV is used. As the cutoff is increased to 500 eV for better accuracy, the second layer is at least 50 meV more favorable than the third. This outcome is consistent with
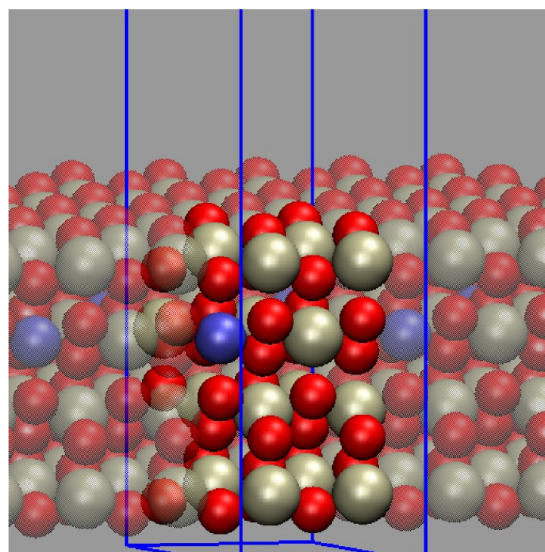
experimental and computational investigations of isolated O vacancies on the (111) CeO$_2$ surface using DFM experiments[65] and DFT + U calculations.[19] It is then concluded that the best position to create a vacancy in a slab model would be on the second O layer with respect to the vacuum direction. The location of this vacancy has to be at a site directly above the dopant atom in doped CeO$_2$.

These results provide neither a reason nor a guarantee for the second layer to remain the most favorable location for a vacancy in doped oxides, as well. Nonetheless, the target quantity E_v^f and, more importantly, the predicted trends are unlikely to be affected in a fundamental way if the vacancy moves and is modeled on a different layer.

3. RESULTS AND DISCUSSIONS

3.1. Calculated Vacancy Energies versus Literature. The energy of O vacancy formation, E_v^f, is calculated for each case of the considered dopants (and pure CeO$_2$) by creating an O vacancy and evaluating the difference in energy before and after creation of the vacancy using

$$E_v^f = E[MCeO_{2-x}] + \frac{1}{2}E[O_2] - E[MCeO_2] \tag{3}$$

Our hypothesis is to correlate E_v^f with the chemical activity of CeO$_2$. Before addressing this hypothesis, we confirm here that E_v^f values from our calculations for doped CeO$_2$ are in agreement with the trends of E_v^f reported in previous computational studies of doped CeO$_2$.[35,37,38,40,44] To this end, we use a slab model for the CeO$_2$ (111) surface and calculate E_v^f in pure as well as in doped CeO$_2$. Figure 8 shows the values calculated here versus those from the literature.

Here, the agreement with the literature should not be judged on the basis of seeking an accumulation around the diagonal line because estimations are dependent on different computational methods. The goal of this comparison is to match not the absolute values of E_v^f for various dopants but the relative ones. It is the relative position of the dopants in Figure 8 that determines the activity of the corresponding compound according to the proposed descriptor.
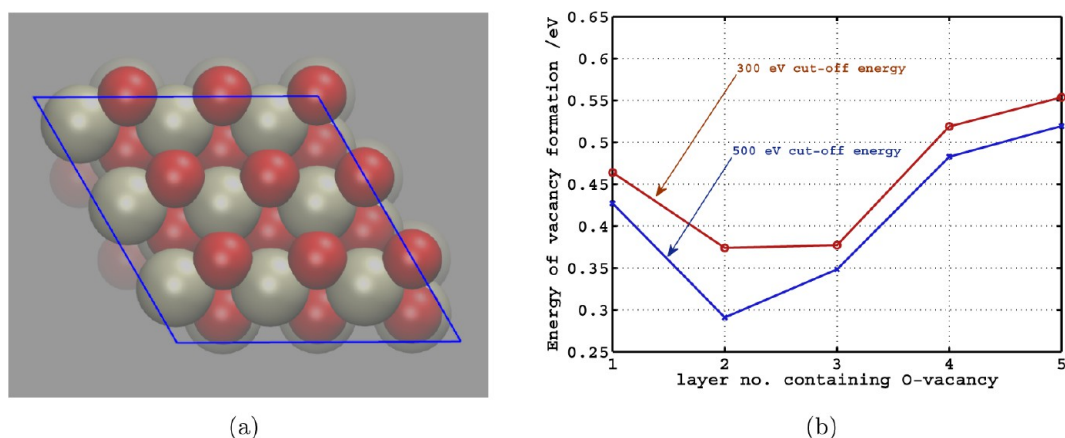
(a)   (b)

Figure 7. Determining the location of the first oxygen vacancy in a slab model of ceria: (a) computational model containing 3 × 3 × 4 trilayers and (b) energetics of vacancy formation versus the layer containing the vacancy. The layer number refers to the layers containing the oxygen atoms with respect to the (111) surface.
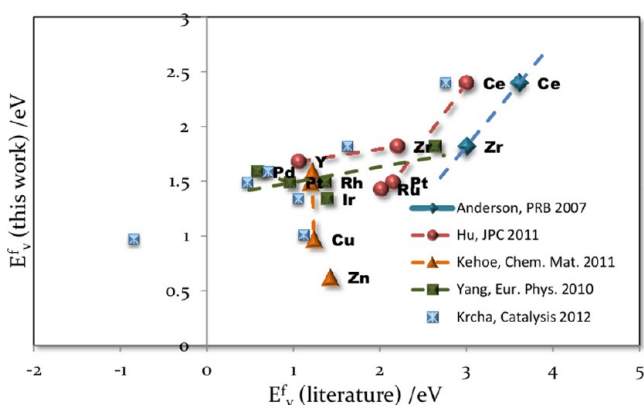

Figure 8. Calculated values of the energy of O vacancy formation for several transition metals as doping elements in the second O layer versus values from the literature.[35,37,38,40,44]

The largest discrepancy between the values calculated in this work exists with the results of Kehoe et al.[40] The trend of E_v^f from Pt and Pd toward Cu and Zn is opposite that of the present calculations. However, it must also be noted that in the same reference, the plot for reduction energy versus ionic radii indicates Zn as an outlier, implying that the E_v^f for Zn might not be completely reliable. Cu has a mixed valency, between 1+ and 2+ and not exactly either of them, which makes it a difficult system to ascertain and the comparison of its values difficult. On the other hand, the trends in values from the present calculations compare really well with the calculated values of Krcha et al.,[38] which is the only other study we found to have also compared the relative trends between several transition metals.

From the comparison of our results with other sources, one can see that the general trend of variation in E_v^f upon doping is the same for all doping elements as well as for undoped CeO_2. This agreement ensures that the model used here to calculate the energy of vacancy formation is reasonably consistent with a wide range of already used models in previous publications. Using either our results or the literature values for E_v^f would leave the discussion and conclusions in the next sections on catalytic activity essentially unaffected if the literature values for various dopants are taken consistently from a particular data set.

Although the above calculations focus on the stoichiometric models, the main issue with DFT + U computations of ceria-based materials is with the nonstoichiometric cases, that is, in cases that the excess electrons localize on the Ce sites. The target quantity of interest in this paper, E_v^f, however, is obtained by subtracting energy values of two systems that are very similar and, thus, unlikely to be affected in large part by further benchmarking.

3.2. Correlation of Activity and Oxygen Vacancy Energy. The term *activity* is used here to refer to the total chemical activity of the ceria compounds when used as a catalyst or cocatalyst. This term, used here to represent the overall result of a chemical mechanism, is not equivalent to the *reducibility* of one system component, at least not in a trivial way. From a general point of view, the chemistry in catalytic systems depends on not only the reducibility of the ceria compounds, or their oxide activity, but also on other factors whose roles are reflected in the chemical mechanism through which the catalytic effects occur. Although the reducibility of a compound is refelected by its ability to release oxygen, there is no guarantee its quantitative value (E_v^f) could undoubtedly be used as the activity descriptor of the corresponding chemistry. Assuming a default equivalence between reducibility and activity implies assuming an equivalence between the whole chemistry of a system, with a possibly complicated mechanism, and one single reaction, an assumption that might not be correct in general and needs to be validated. It is the purpose of this work to show (1) that representing such an unknown or complicated chemical mechanism with one single descriptor is valid for the catalytic activity of CeO_2 in a few studied chemistries and (2) the procedure and the corresponding results of a consistent set of computations to predict that activity.

Instead of dealing with a (probably) complicated or unknown catalytic mechanism, we verify our hypothesis that the calculated values for E_v^f for the first O vacancy in doped CeO_2 correlate well with the chemical activity of the corresponding compounds. The definition of the *activity* of CeO_2 is subject to its application and, hence, is measured generally in a different way in each experimental study. Generally, available results in the literature report activity against variables such as temperature, pressure, composition of catalyst with respect to dopants. Moreover, there is no well-defined unit for measuring the activity of CeO_2. The experiments for measuring even the same kind of activity have been performed by various authors under

different conditions and are thus difficult to compare directly. In most applications, the physical quantity that is supposed to be measured is the reducibility of CeO_2 while playing the role of a catalyst.

In Figure 9, we plot the measured activity of doped CeO_2 from our literature survey toward four reactions: percent CO
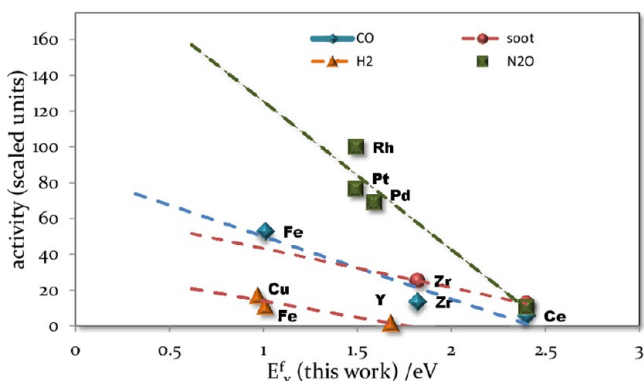

Figure 9. Correlation between the chemical activity of doped ceria in several reactions[23,24,26,66] with the energy of oxygen vacancy formation. For the raw data, refer to the Supporting Information.

conversion,[23] percent soot conversion,[66] maximum H_2 uptake/mV,[24] and percent N_2O conversion.[26] For a measure of activity, we choose values in each case by keeping the value of other variables, such as temperature and compositions, constant while scaling the data by an arbitrary parameter for the convenience of plotting. The original raw data are provided as Supporting Information to this work.

The activity of bulk and doped CeO_2 for all four surveyed reactions indicates a clear correlation with the E_v^f values for transition metal dopants. The linear plots reveal that the activity of CeO_2 increases as E_v^f decreases. The existence of this simple relationship validates the point of this paper in presenting a mechanism-free descriptor for the activity of ceria.

Because the O vacancy forms more easily in the structure, the ceria-based material acts as a better catalyst for all considered processes. The E_v^f values shown in Figure 9 are the result of our calculations, which were shown earlier to be reasonably consistent with the published results. Using literature values for E_v^f does not change the trends of this correlation with the corresponding doped CeO_2 activity if the literature values for various dopants are taken from the same study in a consistent manner. We can thus conclude that E_v^f can be used as an effective computational measure to monitor the activity of doped CeO_2, at least in a relative sense.

The observed linear relationship does not prove a complete and universally valid behavior, since a more complicated relationship is generally expected. In fact, the presence of such a nonlinear relationship has been reported in ref 38, in which a volcano was found for the optimal M/CeO_2 dopant in the methane conversion to CO or CO_2. Despite this valid expectation, the studied experimental results do not reveal any volcano within the range of their measurements conditions. Therefore, the presented descriptor may be applied at least to similar conditions.

Finally, one might argue that other factors (for example, the presence of different catalyst materials in various configurations) can affect the overall activity, as well. We do not rule out such effects. At the same time, one should take into account

the diversity of references used in setting up the observed correlation in Figure 9, which clearly demonstrates a unified picture for the activity of doped ceria. Furthermore, we use this descriptor to predict the effect of doping elements.

3.3. Structural Distortions in Doped CeO_2. Here, we discuss computational results corresponding to relaxed states of the doped CeO_2 slab and the corresponding distortions in the structure upon O vacancy formation. When a dopant atom replaces a Ce ion in the CeO_2 lattice, the periodic electrostatic field distribution changes as a result of a different electronegativity, aliovalency, ionic radius, or a different coordination preference of the dopant with respect to the Ce ion. As a result, significant lattice distortions may occur as a result of structural relaxations and charge relocations. The dopant may even form its own oxide in properly coordinated locations. In several cases, this results in weakened Ce−O bonds, thus, facilitating O vacancy formation.

We observed the change in positions of all O and Ce atoms that are nearest neighbors (NN) to the original location of the O vacancy and the dopant upon O vacancy formation. In all cases, the shift of the Ce atoms from their original locations upon vacancy formation is observed to be less than 0.15 Å. O atoms NN to the vacancy are in the first (surface), third (subsurface; containing vacancy), and fourth layers, and they show comparatively much larger displacements upon vacancy formation; however, the intensity of this distortion varies largely across different dopant elements.

In the case of some dopants (Y, Zr, Rh, and Ir), the O atoms that are NN to the vacancy move mostly in the fourth layer and not so much in the first and third layers (<0.1 Å) upon vacancy formation, but the trend is opposite in others (Pd, Pt). Such trends of preferential movement of O atoms in either the first or fourth layer do not emerge for the case of other dopants studied here, but remarkably, they show much larger distortions overall. For cases (Cu, Fe, and Zn), the NN O atoms close in on the vacancy significantly in both the first and fourth layers, and in addition, there is a discernible movement of O atoms NN to the dopant atom in the sixth layer upon vacancy formation. These observations have been tabulated along with the calculated E_v^f values from our work in Table 1.

Table 1. Average Displacement of O Atoms in Doped CeO_2 versus the Oxygen Layer Neighboring the Vacany[a]

dopant	L-1 (NN to vac)	L-3 (NN to vac)	L-4 (NN to vac)	L-6 (NN to M)	E_v^f (eV)
Pt	0.34				1.48
Pd	0.32				1.58
Y			0.27		1.68
Zr			0.34		1.82
Rh			0.38		1.49
Ir			0.43		1.34
Ru			0.73	0.59	1.75
Fe	0.20	0.27	0.77	0.69	1.01
Cu	0.24		0.26	0.24	0.98
Zn	0.27		0.37	0.40	0.62

[a]All mentioned values except for the last column are average values in angstroms. Only displacements of more than >0.1 Å are reported.

A correlation between structural distortions and energy values for O vacancy formation for the compared cases can be seen within the groups, which are separated by horizontal lines in Table 1, and also, to a certain extent, among the groups.

The grouping in the Table is based on the dominant distortion in the position of the oxygen atoms based on their distance to the vacancy location. Trends within dopant groups (Y, Rh, and Ir) and (Pt and Pd) can be observed because the dopant with the lower E_v^f has a higher degree of distortion among these, with Zr appearing as an outlier. Likewise, Cu, Zn, and Fe show much larger distortions in their structure upon vacancy formation as compared with the other dopants and have significantly lower E_v^f values, whereas Ru comes up as an exception. In principle, these findings are quite consistent with previous modeling studies,[36,42,44] which emphasize that structural relaxations after vacancy formation are crucial to the energetics in doped CeO_2.

3.4. Electronic Effects and Charge Compensation. The substitution of a Ce atom in a CeO_2 system with an aliovalent dopant, which has a lower formal oxidation state than that of cerium(4+), creates unoccupied 2p states on the oxygen atoms neighboring the site of substitution. These partially unfilled O atoms (O−), in the polaron state[67] lack a closed shell as in O(2−) and are less stable. To compensate for the unoccupied 2p states, an oxygen vacancy forms on the surface (or bulk) thus leaving excess electrons, which are localized on cerium and oxygen ions, depending on the oxidation state and the coordination preference of the dopant cation. This mechanism of vacancy formation, termed charge compensating oxygen vacancy formation,[67] has also been observed in experimental studies.[68]

Studies of CeO_2 surfaces with substitutional doping with divalent[39] and trivalent[47] cations report that for quite a few cases of dopants, the charge compensation effect is strong enough to make the formation of the first oxygen vacancy spontaneous, that is, a negative energy of vacancy formation. Apart from the charge compensation effect, the lowering in the vacancy formation energy was explained in terms of the distortions induced due to the mismatch of the ionic radii or due to the coordination preference. In another study of Cu-doped bulk CeO_2 bulk,[69] a significant lowering in energy of the first oxygen formation has been also reported. In addition, the dopant was observed to reduce the vacancy formation energy for the second vacancy, which does not occur via charge compensation. They proposed that electronic effects due to the charge compensation only partially lower the vacancy formation energy, and half of the reduction in formation energy can be attributed to the relaxations introduced by doping. However, there are no major reports of spontaneous vacancy formation for the first oxygen vacancy. It must be noted that in ref47, two dopants instead of one were used on the same supercell neighboring to each other. That configuration, according to the above discussions, is potentially unstable and might lead to the creation of a spontaneous oxygen vacancy.

From a charge point of view, on the basis of a Bader charge analysis, the cases analyzed in this study do not show any significant change in the oxidation state of the dopants upon vacancy formation. The observation is in agreement with the study by Lu et al.[69] Indeed, the aliovalency of the dopant cations affects the oxygen vacancy formation energy depending on two factors: (i) the concentration and (ii) the oxidation state of the dopant atoms (2+ or 3+, for example). If there are more dopants, then more O− polarons will be created, and if the oxidation state of the dopant is 2+ instead of 3+, two polarons from just one dopant will be formed. With a higher number of O− polarons in neighboring positions, there will be a higher tendency in the system to form an oxygen vacancy, and thus, the energy of oxygen vacancy formation will be lower.

The current results fit this description of the charge compensation process well because it is seen by correlating the vacancy formation energies with the oxidation state of the dopants.

There are contributing factors other than the oxidation state, such as electronegativity; ionic radii; and in particular, the structural distortions. The present results, however, show that the oxidation state plays a major role in determining the vacancy formation energy. Dopants (such as Cu, Zn, and Fe) that are generally found in lower oxidation states tend to have a lower energy for the vacancy formation than dopants (such as Ru, Rh, Y, Ir, and Zr) with comparatively higher oxidation states. This can be explained in terms of charge compensation: when a dopant with oxidation state of 2+ is introduced at a cerium site, it creates two polaron states (O−) with unfilled 2p states, but when a dopant with oxidation state 3+ is introduced, a single polaron state is created. The charge compensation effect is then much stronger in the case of the lower oxidation state dopants because of the possibility of more stabilization upon vacancy formation.

3.5. Prediction of CeO_2 Activity upon Doping. Finally, we summarize our current findings for doped ceria by plotting E_v^f for several transition metals in Figure 10. On the basis of the
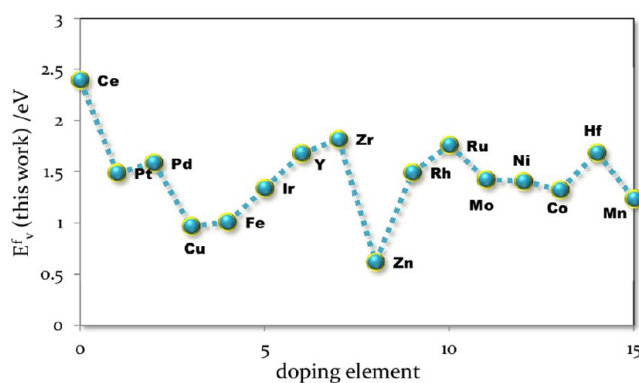

Figure 10. Calculated values of energy of O vacancy formation for several transition metals as doping elements in the second O layer.

proposed measure of activity, pure ceria has the lowest activity because its E_v^f is highest among all doped compounds. Doping ceria with Zn is suggested to have the highest activity, and the rest of the candidate-doping elements reside somewhere between the pure and the Zn-doped ceria. However, Zn may not be the best dopant because of uncertainties over its doping effect in ceria.

In a study on the role of lattice distortions in the OSC of doped CeO_2 by Kehoe et al.,[40] it was argued that despite having an ionic radius similar to that of Pt, Zn does not lower the value of oxygen vacancy formation energy as much as Pt because in contrast to Pt, it does not cause enough distortions in the host oxide structure, which results in a lower E_v^f. Another study on the crystal field stabilization of dopant ions in CeO_2 by Scanlon et al.[42] reports that Zn is not a suitable dopant because it cannot take a square planar configuration, but actually distorts to form four long and four short Zn−O bonds in a tetrahedral coordination environment.

Our observations on the structural distortions are consistent with the work of Scanlon et al.[42] and in agreement with the hypothesis of Kehoe et al.[40] that larger structural distortions result in lower E_v^f. In addition, a very low value of energy for the

vacancy formation in the case of Zn-doped ceria has been reported recently by a comparative study of the doping effect of several transition metals on the CeO_2 (111) surface.[38] In the literature, a clear understanding of or agreement on why Zn is not a suitable dopant is still missing. Owing to the lack of experimental evidence and conceptual disagreements between various studies, we conclude that the effect of Zn as a dopant in CeO_2 is yet unclear.

In summary, our computations in Figure 10 point to Cu and Fe among the set of considered dopants as the most promising elements to increase the activity of ceria in catalytic reactions. Further theoretical and experimental results are necessary to monitor the activity of specific combinations of doping elements and the overall activities toward specific applications.

4. CONCLUSIONS

We performed a comprehensive literature survey on the structure, surfaces, and the activity properties of ceria and its doped compounds. Our calculations for several characteristics of bulk, surface energies, and computational parameters were benchmarked against both computational and experimental literature results. We presented the basic structural scenarios that may emerge in the distribution of a dopant on ceria surfaces and for further analysis, we chose the case in which the dopant atoms replace a Ce atom in the ceria lattice.

Our estimations for the formation energy of an O vacancy predict relative values for various dopants that are in good general agreement with results published previously using different computational models. Hence, our conclusions about the activity of ceria, which are based on this energy quantity, will not be affected if literature values pertaining to a consistent data set are used instead of ours.

Most importantly, we tested and verified our hypothesis that oxygen vacancy formation in doped ceria correlates clearly with the chemical activity of this oxide. It was shown that this hypothesis is, indeed, valid: because the vacancy forms more easily, the ceria-based compounds become more active toward CO, H_2, soot, and N_2O reactions and perhaps toward other reactions, as well.

We applied the presented activity descriptor to predict activity of doped ceria. On the basis of the calculated values of energy for O vacancy formation and structural relaxations, we propose that doping CeO_2 with Cu or Fe can significantly enhance the activity of ceria. This new activity descriptor might play a similar role in other chemical catalytic systems. Another feature of the presented descriptor is to establish a mechanism-free approach to predict activity, which accelerates the optimization of ceria-based compounds, at least in the studied scenario.

ASSOCIATED CONTENT

Ⓢ Supporting Information

Additional experimental details and data and additional references. This material is available free of charge via the Internet at http://pubs.acs.org.

AUTHOR INFORMATION

Corresponding Author

*E-mail: masoud@stanfordalumni.org.

Notes

The authors declare no competing financial interest.

ACKNOWLEDGMENTS

REFERENCES

(1) Azzam, K. G.; Babich, I. V.; Seshan, K.; Lefferts, L. *J. Catal.* **2007**, *251* (1), 153−162.

(2) Huang, Y.; Wang, A.; Li, L.; Wang, X.; Su, D.; Zhang, T. *J. Catal.* **2008**, *255* (2), 144−152.

(3) Li, W.; Gracia, F. J.; Wolf, E. E. *Catal. Today* **2003**, *81* (3), 437−447.

(4) Kaspar, J.; Fornasiero, P.; Graziani, M. *Catal. Today* **1999**, *50* (2), 285−298.

(5) Dresselhaus, M. S.; Thomas, I. L. *Nature* **2001**, *414*, 332−337.

(6) Murray, E. P.; Tsai, T.; Barnett, S. A. *Nature* **1999**, *400*, 649.

(7) Diwell, A. F.; Rajaram, R. R.; Shaw, H. A.; Truex, T. J. *The Role of Ceria in Three-Way Catalysts*; Elsevier Science Publishers BV: Amsterdam, The Netherlands, 1991; Vol. 71.

(8) Bera, P.; Gayen, A.; Hegde, M. S.; Lalla, N. P.; Spadaro, L.; Frusteri, F.; Arena, F. *J. Phys. Chem. B* **2003**, *107* (25), 6122−6130.

(9) Nagai, Y.; Hirabayashi, T.; Dohmae, K.; Takagi, N.; Minami, T.; Shinjoh, H.; Matsumoto, S. *J. Catal.* **2006**, *242* (1), 103−109.

(10) Dictor, R.; Roberts, S. *J. Phys. Chem.* **1989**, *93* (15), 5846−5850.

(11) Trovarelli, A.; de Leitenburg, C.; Boaro, M.; Dolcetti, G. *Catal. Today* **1999**, *50* (2), 353−367.

(12) Wuilloud, E.; Delley, B.; Schneider, W. D.; Baer, Y. *Phys. Rev. Lett.* **1984**, *53* (2), 202−205.

(13) Marabelli, F.; Wachter, P. *Phys. Rev. B: Condens. Matter* **1987**, *36* (2), 1238−1243.

(14) Mullins, D. R.; Overbury, S. H.; Huntley, D. R. *Surf. Sci.* **1998**, *409* (2), 307−319.

(15) Henderson, M. A.; Perkins, C. L.; Engelhard, M. H.; Thevuthasan, S.; Peden, C. H. F. *Surf. Sci.* **2003**, *526* (1), 1−18.

(16) Shao, X.; Jerratsch, J. F.; Nilius, N.; Freund, H. J. *Phys. Chem. Chem. Phys.* **2011**, *13* (27), 12646−12651.

(17) Esch, F.; Fabris, S.; Zhou, L.; Montini, T.; Africh, C.; Fornasiero, P.; Comelli, G.; Rosei, R. *Science* **2005**, *309* (5735), 752−755.

(18) Jerratsch, J. F.; Shao, X.; Nilius, N.; Freund, H. J.; Popa, C.; Ganduglia-Pirovano, M. V.; Burow, A. M.; Sauer, J. *Phys. Rev. Lett.* **2011**, *106* (24), 246801.

(19) Zhang, C.; Michaelides, A.; King, D. A.; Jenkins, S. J. *Phys. Rev. B* **2009**, *79*, 075433.

(20) Bedrane, S.; Descorme, C.; Duprez, D. *Catal. Today* **2002**, *75* (1−4), 401−405.

(21) Mullins, D. R.; Overbury, S. H. *Surf. Sci.* **2002**, *511* (1), L293−L297.

(22) Liu, Y.; Wen, C.; Guo, Y.; Lu, G.; Wang, Y. *J. Phys. Chem. C* **2010**, *114* (21), 9889−9897.

(23) Laguna, O. H.; Romero Sarria, F.; Centeno, M. A.; Odriozola, J. A. *J. Catal.* **2010**, *276* (2), 360−370.

(24) Gupta, A.; Waghmare, U. V.; Hegde, M. S. *Chem. Mater.* **2010**, *22* (18), 5184−5198.

(25) Panagiotopoulou, P.; Kondarides, D. I. *Catal. Today* **2006**, *112* (1−4), 49−52.

(26) Parres-Esclapez, S.; Illán-Gómez, M. J.; de Lecea, C.; Bueno-López, A. *Appl. Catal., B* **2010**, *96* (3), 370−378.

(27) Gennard, S.; Cora, F.; Catlow, C. R. A. *J. Phys. Chem. B* **1999**, *103* (46), 10158−10170.

(28) Migani, A.; Neyman, K. M.; IIlas, F.; Bromley, S. T. *J. Chem. Phys.* **2009**, *131* (6), 64701.

(29) Yang, Z.; Woo, T. K.; Baudin, M.; Hermansson, K. *J. Chem. Phys.* **2004**, *120* (16), 7741−7749.

(30) Nolan, M.; Grigoleit, S.; Sayle, D. C.; Parker, S. C.; Watson, G. W. *Surf. Sci.* **2005**, *576* (1−3), 217−229.

(31) Fabris, S.; de Gironcoli, S.; Baroni, S.; Vicario, G.; Balducci, G. *Phys. Rev. B* **2005**, *71* (4), 237102.

(32) Andersson, D. A.; Simak, S. I.; Johansson, B.; Abrikosov, I. A.; Skorodumova, N. V. *Phys. Rev. B* **2007**, *75* (3), 035109.

(33) Castleton, C. W. M.; Kullgren, J.; Hermansson, K. *J. Chem. Phys.* **2007**, *127* (24), 244704.

(34) Loschen, C.; Carrasco, J.; Neyman, K.; Illas, F. *Phys. Rev. B* **2007**, *75* (3), 035115.

(35) Andersson, D. A.; Simak, S. I.; Skorodumova, N. V.; Abrikosov, I. A.; Johansson, B. *Phys. Rev. B* **2007**, *76* (17), 174119.

(36) Wang, H. F.; Gong, X. Q.; Guo, Y. L.; Guo, Y.; Lu, G. Z.; Hu, P. *J. Phys. Chem. C* **2009**, *113* (23), 10229−10232.

(37) Hu, Z.; Metiu, H. *J. Phys. Chem. C* **2011**, *115* (36), 17898−17909.

(38) Krcha, M. D.; Mayernick, A. D.; Janik, M. J. *J. Catal.* **2012**, *293* (0), 103−115.

(39) Nolan, M. *J. Mater. Chem.* **2011**, *21* (25), 9160−9168.

(40) Kehoe, A. B.; Scanlon, D. O.; Watson, G. W. *Chem. Mater.* **2011**, *23*, 4464.

(41) Mayernick, A. D.; Janik, M. J. *J. Chem. Phys.* **2009**, *131*, 084701.

(42) Scanlon, D. O.; Morgan, B. J.; Watson, G. W. *Phys. Chem. Chem. Phys.* **2011**, *13* (10), 4279−4284.

(43) Yang, Z.; Luo, G.; Lu, Z.; Woo, T. K.; Hermansson, K. *J. Phys.: Condens. Matter* **2008**, *20*, 035210.

(44) Yang, Z. X.; Ma, D. W.; Yu, X. H.; Hermansson, K. *Eur. Phys. J., B: Condens. Matter Complex Syst.* **2010**, *77* (3), 373−380.

(45) Liu, Z.; Jenkins, S. J.; King, D. A. *Phys. Rev. Lett.* **2005**, *94*, 196102.

(46) Zhang, C.; Michaelides, A.; King, D. A.; Jenkins, S. J. *J. Phys. Chem. C* **2009**, *113* (16), 6411−6417.

(47) Nolan, M. *J. Phys. Chem. C* **2011**, *115* (14), 6671−6681.

(48) Nolan, M. *Chem. Phys. Lett.* **2010**, *492* (1), 115−118.

(49) Kresse, G.; Försth, M. *VASP Manual*; 2003; pp 58−59.

(50) Burke, K.; Perdew, J. P.; Ernzerhof, M. *Phys. Rev. Lett.* **1996**, *77*, 3865.

(51) Burke, K.; Perdew, J. P.; Ernzerhof, M. *Phys. Rev. Lett.* **1997**, *78*, 1396.

(52) Da Silva, J. L. F.; Ganduglia-Pirovano, M. V.; Sauer, J.; Bayer, V.; Kresse, G. *Phys. Rev. B* **2007**, *75*, 045121.

(53) Plata, J. J.; Márquez, A. M.; Sanz, J. F. *J. Chem. Phys.* **2012**, *136* (4), 1101.

(54) Janesko, B. G.; Henderson, T. M.; Scuseria, G. E. *Phys. Chem. Chem. Phys.* **2009**, *11*, 443−454.

(55) Henderson, T. M.; Paier, J.; Scuseria, G. E. *Phys. Status Solidi B* **2011**, *248* (4), 767−774.

(56) Tasker, P. W. *J. Phys. C: Solid State Phys.* **1979**, *12*, 4977.

(57) Nörenberg, H.; Briggs, G. A. D. *Phys. Rev. Lett.* **1997**, *79* (21), 4222.

(58) Nörenberg, H.; Harding, J. H. *Surf. Sci.* **2001**, *477* (1), 17−24.

(59) Namai, Y.; Fukui, K.; Iwasawa, Y. *J. Phys. Chem. B* **2003**, *107* (42), 11666−11673.

(60) Herman, G. S. *Phys. Rev. B* **1999**, *59* (23), 14899.

(61) Mullins, D. R.; Radulovic, P. V.; Overbury, S. H. *Surf. Sci.* **1999**, *429* (1), 186−198.

(62) Nörenberg, H.; Briggs, G. A. D. *Surf. Sci.* **1999**, *433*, 127−130.

(63) Tasker, P. W. *J. Phys. Coll.* **1980**, *41* (C6), 6−6.

(64) Kümmerle, E. A.; Heger, G. *J. Solid State Chem.* **1999**, *147* (2), 485−500.

(65) Torbrügge, S.; Reichling, M.; Ishiyama, A.; Morita, S.; Custance, Ó. *Phys. Rev. Lett.* **2007**, *99*, 056101.

(66) Katta, L.; Sudarsanam, P.; Thrimurthulu, G.; Reddy, B. M. *Appl. Catal., B* **2010**, *101* (1), 101−108.

(67) Iwaszuk, A.; Nolan, M. *J. Phys.: Condens. Matter* **2011**, *23*, 334207.

(68) Shen, M.; Wang, J.; Shang, J.; An, Y.; Wang, J.; Wang, W. *J. Phys. Chem. C* **2009**, *113*, 1543−1551.

(69) Lu, Z.; Yang, Z.; He, B.; Castleton, C.; Hermansson, K. *Chem. Phys. Lett.* **2011**, *510*, 60−66.